

Isolation and Characterization of Fluorescent Nanoparticles from Pristine and Oxidized Electric Arc-Produced Single-Walled Carbon Nanotubes

Massimo Bottini,[†] Chidambara Balasubramanian,[‡] Marcia I. Dawson,[†] Antonio Bergamaschi,[§] Stefano Bellucci,[‡] and Tomas Mustelin^{*,†}

Burnham Institute for Medical Research, 10901 North Torrey Pines Road, La Jolla, California 92037, INFN, Laboratori Nazionali di Frascati, Via E. Fermi 40, 00044, Frascati, Italy, and Department of Environmental, Occupational and Social Medicine, University of Rome Tor Vergata, Via Montpellier 1, 00133 Rome, Italy

Received: September 27, 2005; In Final Form: November 3, 2005

Fluorescent nanoparticles were isolated from both pristine and nitric acid-oxidized commercially available carbon nanotubes that had been produced by an electric arc method. The pristine and oxidized carbon nanotube-derived fluorescent nanoparticles exhibited a molecular-weight-dependent photoluminescence in the violet-blue and blue to yellowish-green ranges, respectively. The molecular weight dependency of the photoluminescence was strongly related to the specific supplier. We analyzed the composition and morphology of the fluorescent nanoparticles derived from pristine and oxidized nanotubes from one supplier. We found that the isolated fluorescent materials were mainly composed of calcium and zinc. Moreover, the pristine carbon nanotube-derived fluorescent nanoparticles were hydrophobic and had a narrow distribution of maximal lateral dimension. In contrast, the oxidized carbon nanotube-derived fluorescent nanoparticles were superficially oxidized and/or coated by a thin carbon layer, had the ability to aggregate when dispersed in water, and exhibited a broader distribution of maximal lateral dimension.

1. Introduction

Since their discovery, carbon nanotubes (CNT) have been intensely investigated because of their unique physical and chemical properties and their potential usage in medical and biotechnological applications.¹ For these uses, a high level of purity is required to avoid undesired toxic effects from impurities. Contaminants in CNT have been classified as carbonaceous (amorphous carbon and graphitic nanoparticles) and metallic (typically from transition metal catalysts used in their synthesis). Recently, electrophoresis of nitric acid-oxidized electric arc-produced CNT was used to separate tubular carbon from fluorescent nanoparticle (FP) contaminants, which demonstrated a molecular weight (MW)-dependent photoluminescence and did not contain metal residue from the catalysts.² Here we report the characterization of fluorescent materials isolated from both pristine (p) and nitric-acid-oxidized (ox) arc-produced CNT received from different suppliers.³ The FP were separated from CNT by ultracentrifugation of nanotubes dispersed in a 1% aqueous solution of the surfactant sodium dodecyl sulfate (SDS). The FP, which remained in the supernates, were characterized by absorbance, fluorescence, and electron dispersive X-ray (EDX) spectroscopies, scanning electron microscopy (SEM), and high-resolution transmission electron microscopy (HRTEM).

2. Experimental Section

2.1. Materials. Carbon black and graphite were provided by Solution Dispersions, Inc. (Cynthiana, KY). Samples of pCNT and oxCNT were purchased from Carbon Solutions, Inc.

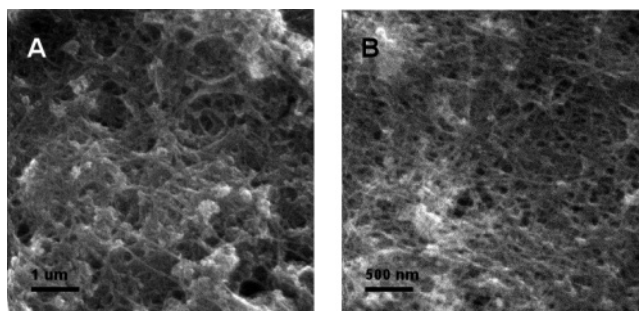


Figure 1. SEM images of pristine (A) and oxidized (B) carbon nanotube samples from Carbon Solutions, Inc.

(Riverside, CA) and Nanocs, Inc. (New York, NY). The pCNT from Carbon Solutions, Inc. were purified by air oxidation, closely approximated the pristine state, and had 80 wt % carbonaceous purity and approximately 10 wt % metallic impurities.⁴ An SEM image of this material is shown in Figure 1A. The oxCNT from Carbon Solutions, Inc. (Figure 1B) were treated with hot nitric acid.⁵ They had 83 wt % carbonaceous purity, approximately 10 wt % metallic contaminants, and contained approximately 4 mmol/g of carboxylic acid groups. Both pristine and oxidized CNT from Nanocs, Inc. had a carbonaceous purity around 85 wt %. The oxCNT had approximately 0.4 mmol/g of carboxylic acid groups. A sample of pCNT was also purchased from Carboxex, Inc. (Broomall, PA). It had a carbonaceous purity around 60 wt % and approximately 30 wt % metallic contaminants.

2.2. Methods. Samples of graphite, carbon black, and CNT were dispersed in 1% SDS (1 mg/mL) by sonication for 5 min using a cup-horn sonicator (10 W) (Misonix, Inc., Farmingdale, NY). A 10-mL aliquot of each dispersion was immediately ultracentrifuged for 4 h at 120 000g (Beckman Optima XL-80K ultracentrifuge, Palo Alto, CA). The supernates (ap-

* Corresponding author. Fax: (858) 713-6274. Phone: (858) 713-6270. E-mail: tmustelin@burnham-inst.org.

[†] Burnham Institute for Medical Research.

[‡] INFN, Laboratori Nazionali di Frascati.

[§] University of Rome Tor Vergata.

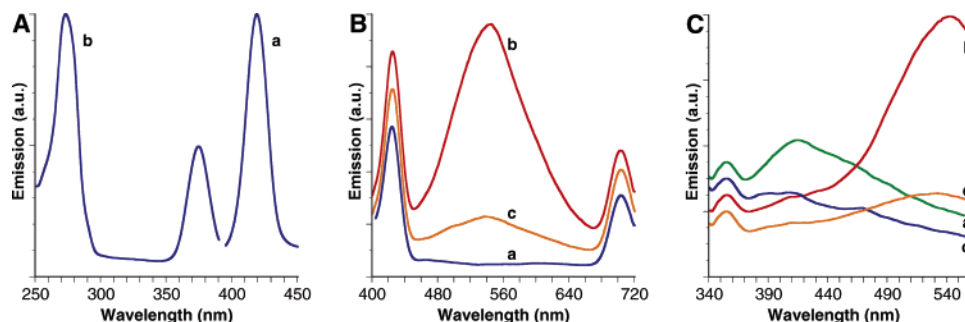


Figure 2. Spectroscopic features of graphite, carbon black (from Solution Dispersions, Inc.), and CNT samples from Carbon Solutions, Inc. (A) Emission (trace a) and excitation (trace b) spectra of graphite dispersed in 1% aqueous SDS. (B) Emission spectra, upon excitation at 375 nm, of graphite (trace a) and oxCNT (trace b) dispersed in 1% aqueous SDS and of oxCNT in pure water (trace c). (C) Emission spectra, upon excitation at 315 nm, of pCNT (trace a), oxCNT (trace b), and graphite (trace c) dispersed in 1% aqueous SDS and of oxCNT in pure water (trace d).

proximately 9 mL) were carefully decanted from the pellet, sonicated for 5 min, and then sequentially ultrafiltered through a centrifugal filter device using four nominal molecular weight cutoff membranes (Microcon, Millipore, Bedford, MA) to give <3, 3–10, 10–30, and 30–100 kDa fractions. CNT (Carbon Solutions, Inc.) in water were also treated as mentioned above in order to release the FP.

2.3. Instrumental Analysis. Absorbance (UV–vis spectrophotometer model 8453, Agilent Technologies, Palo Alto, CA) and fluorescence (MOS-250 fluorescence spectrometer, Bio-Logic, Claix, France) spectra and EDX analysis (200 keV beam energy, JEOL 2000, Tokyo, Japan) were used for characterization.

3. Results

3.1. Graphite, Carbon Black, and Carbon Nanotubes from Carbon Solutions, Inc. For comparison purposes, the spectroscopic behavior of graphite and carbon black dispersions in SDS were initially examined. Upon excitation at 276 nm, both dispersions exhibited a strong fluorescence emission at 420 nm (Figure 2A, trace a). Excitation at the 420-nm emission wavelength produced peaks at 276 and 375 nm (Figure 2A, trace b). Excitation at 375 nm produced fluorescent peaks at 426 and 703 nm (Figure 2B, trace a).

Upon excitation at 276 nm, pCNT and oxCNT in SDS emitted a 420-nm peak. In addition, with excitation at 375 nm, only oxCNT produced a strong, broad 544-nm peak (Figure 2B, trace b). The excitation spectrum for oxCNT, which was obtained by monitoring the 544-nm emission, showed a 365-nm peak with a 315-nm shoulder. Excitation of pCNT and oxCNT at 315 nm produced 425- and 544-nm photoluminescent peaks (Figure 2C, traces a and b), respectively. In contrast, excitation of graphite and carbon black dispersions at 315 nm only produced three weak peaks at approximately 385, 408, and 467 nm (Figure 1C, trace c). Excitation of the aqueous oxCNT dispersion at 315 and 375 nm produced weaker and slightly blue-shifted maxima (Figure 2C, trace d, and Figure 2B, trace c, respectively) compared to those of the supernate from oxCNT in SDS.

Excitation of the clear grayish pCNT-in-SDS-derived supernate at 315 nm (Figure 3A, trace a) produced a 423-nm emission peak (Figure 3A, trace b), while excitation at 365 nm produced two weak peaks at 415 and 486 nm (Figure 3A, trace c, magnification approximately 5 \times). Excitation of the clear brownish oxCNT-in-SDS-derived supernate at 315 and 365 nm (Figure 3B, trace a) produced the same (540 nm) photoluminescent peak (Figure 3B, trace b). The supernate from the aqueous pCNT dispersion did not fluoresce. In contrast, 315- or 365-nm excitation of the oxCNT-in-water-derived supernate

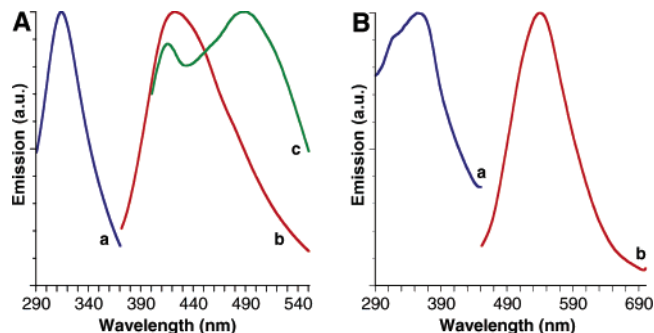


Figure 3. Spectroscopic features of supernates obtained by ultracentrifugation of CNT samples from Carbon Solutions, Inc. (A) Normalized excitation (trace a) and emission (traces b and c) spectra of the supernate obtained by centrifugation of pCNT dispersed in 1% SDS. (B) Normalized excitation (trace a) and emission (trace b) spectra of the supernate obtained by centrifugation of oxCNT dispersed in 1% SDS.

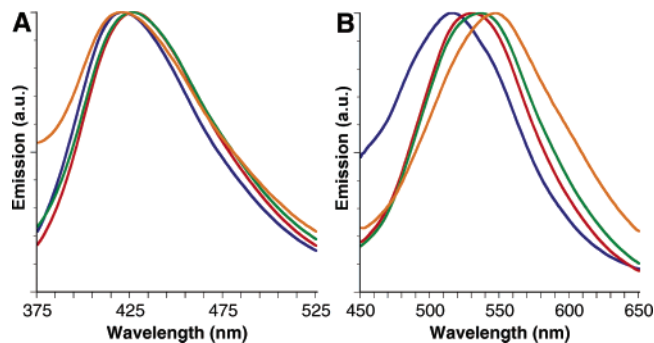


Figure 4. Normalized emission spectra of the supernatant fractions obtained by ultrafiltration through nominal molecular weight cutoff membranes (blue, <3 kDa; red, 3–10 kDa; green, 10–30 kDa; orange, 30–100 kDa) of pCNT (A) and oxCNT (B) samples from Carbon Solutions, Inc.

produced weaker, slightly blue-shifted emission maxima compared to those from oxCNT-in-SDS-derived supernate with matching absorption at the excitation wavelengths.

Interestingly, the nominal MW cutoff fractions from the pCNT and oxCNT supernates exhibited MW-dependent spectroscopic features. CNT were absent from all fractions on the basis of their lack of CNT visible absorptions. Upon excitation at 315 nm, the pCNT-derived supernatant fractions below 30 kDa MW exhibited fluorescent peaks having maxima within a 5-nm range (421–426 nm) and full-width at half-maxima (fwhm) that increased with molecular weight (Figure 4A and Table 1). In contrast, the 30–100 kDa fraction produced a weaker and broader 420-nm peak compared to the fluorescent peaks of the other fractions with matching absorption at the 315-nm excitation wavelength (Figure 4A and Table 1). Upon

TABLE 1: Emission Peak Wavelength (λ_{em}) and Full-Width at Half-Maxima (fwhm) of the Supernates and the Nominal Molecular Weight Cutoff Fractions Isolated from PCNT and OxCNT Samples from Carbon Solutions, Inc

sample ^a	pCNT ($\lambda_{ex} = 315$ nm)		oxCNT ($\lambda_{ex} = 365$ nm)	
	λ_{em} (nm)	fwhm (nm)	λ_{em} (nm)	fwhm (nm)
supernate	423	93	540	103
fractionated	420	100 \pm 2 ^b	547	120
supernate	425	87	537	105
3–10 kDa	426	82	530	99
<3 kDa	421	81	516	153

^a Supernates obtained by ultracentrifugation at 120 000g and then fractionated by ultrafiltration. ^b Extrapolated value.

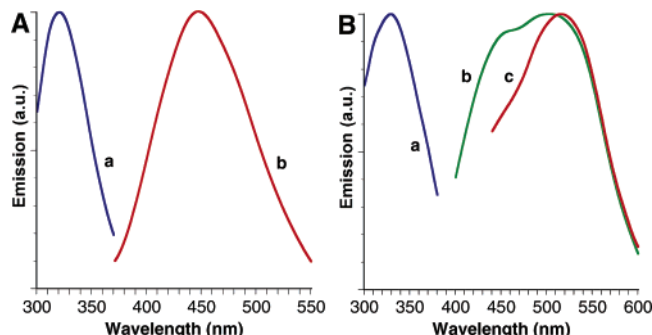


Figure 5. Spectroscopic features of supernates obtained by ultracentrifugation of CNT samples from Nanocs, Inc. (A) Normalized excitation (trace a) and emission (trace b) spectra of the supernate obtained by ultracentrifugation of pCNT dispersed in 1% SDS. (B) Normalized excitation (trace a) and emission (traces b and c) spectra of the supernate obtained by ultracentrifugation of oxCNT dispersed in 1% SDS.

excitation at 365 nm, all fractions exhibited the same weak, broad peaks centered at approximately 415 and 486 nm.

In addition, the photoemission spectra produced by oxCNT-in-SDS-derived supernatant fractions was progressively red-shifted with increasing molecular weight (Figure 4B and Table 1). Only the fraction below 3 kDa exhibited a broad emission spectrum that suggested a contribution from the violet range. Upon excitation of this fraction at 315 nm, a distinct shoulder at 425 nm appeared. The spectra from the oxCNT-in-water-derived supernatant fractions showed weaker and blue-shifted emission peaks compared to those of oxCNT-in-SDS-derived fractions with matching absorption at the same excitation wavelength.

3.2. Carbon Nanotubes from Nanocs, Inc. Upon excitation at 276 nm, pCNT and oxCNT in SDS emitted a 420-nm peak. Upon excitation at 315 nm, pCNT produced a 450-nm peak. The excitation spectrum for pCNT, which was obtained by monitoring the 450-nm emission, showed a 320-nm peak. Upon excitation at 315 nm, oxCNT produced a broad peak centered at approximately 470 nm with intense shoulders at 450 and approximately 520 nm. The excitation spectrum for oxCNT, which was obtained by monitoring the 470-nm emission, showed a 330-nm peak with shoulders at 320 and 365 nm.

Excitation of the clear grayish pCNT-in-SDS-derived supernate at 320 nm (Figure 5A, trace a) produced a 447-nm emission peak (Figure 5A, trace b). Excitation at 365 nm produced two weak peaks at 417 and 478 nm. Excitation of the clear brownish oxCNT-in-SDS-derived supernate at 320 and 330 nm produced the same broad 503-nm peak with an intense shoulder approximately at 450 nm (Figure 5B, trace b). In contrast, excitation at 365 nm produced a 515-nm peak (Figure 5B, trace c).

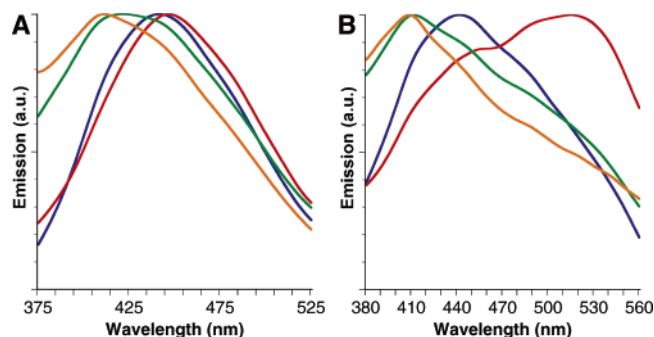


Figure 6. Normalized emission spectra of the supernatant fractions obtained by ultrafiltration through nominal molecular weight cutoff membranes (blue, <3 kDa; red, 3–10 kDa; green, 10–30 kDa; orange, 30–100 kDa) of pCNT (A) and oxCNT (B) samples from Nanocs, Inc.

TABLE 2: Emission Peak Wavelength (λ_{em}) of the Supernates and the Nominal Molecular Weight Cutoff Fractions Isolated from PCNT and OxCNT from Nanocs, Inc

sample ^a	λ_{em} (nm)	
	pCNT ($\lambda_{ex} = 320$ nm)	oxCNT ($\lambda_{ex} = 330$ nm)
supernate	447	503
fractionated	411	409
supernate	421	412
3–10 kDa	447	515
<3 kDa	442	442

^a Supernates obtained by ultracentrifugation at 120 000g and then fractionated by ultrafiltration.

The nominal MW cutoff fractions from the pCNT and oxCNT supernates exhibited strongly MW-dependent spectroscopic features. CNT were absent from all fractions on the basis of their lack of CNT visible absorptions. Upon excitation at 320 nm, the below 3 kDa and the 3–10 kDa pCNT-derived supernatant fractions exhibited fluorescent peaks having maxima at 442 and 447 nm, respectively (Figure 6A and Table 2). In contrast, the 10–30 and 30–100 kDa fractions produced weaker and broader peaks, centered at 421 and 411 nm, respectively, compared to the fluorescent peaks of the other fractions with matching absorption at the 320-nm excitation wavelength (Figure 6A and Table 2). Upon excitation at 365 nm, all fractions exhibited the same weak, broad peaks centered at approximately 417 and 478 nm.

Upon excitation at 330 nm the below 3 kDa oxCNT-derived supernatant fraction exhibited a 442-nm peak with a shoulder at approximately 485 nm, whereas the 3–10 kDa fraction exhibited a 515 nm peak with shoulders at approximately 455 (major) and 485 (minor) nm (Figure 6B and Table 2). In contrast, the 10–30 and 30–100 kDa fractions produced weaker peaks, centered at 412 and 409 nm, respectively, compared to the fluorescent peaks of the other fractions with matching absorption at the 330-nm excitation wavelength (Figure 6B and Table 2). Upon excitation at 320 nm all the fractions revealed the same spectroscopic features as observed with the 330-nm excitation. Upon excitation at 365 nm only the 3–10 kDa fraction revealed an intense 515-nm peak, whereas the other fractions revealed weaker spectroscopic features.

3.3. Carbon Nanotubes from Carboxyl, Inc. Upon excitation at 276 nm, pCNT in SDS emitted a 420-nm peak. Upon excitation at 315 nm, pCNT produced a peak at approximately 415 nm. The excitation spectrum for pCNT, which was obtained by monitoring the 415-nm emission, showed a 335-nm peak.

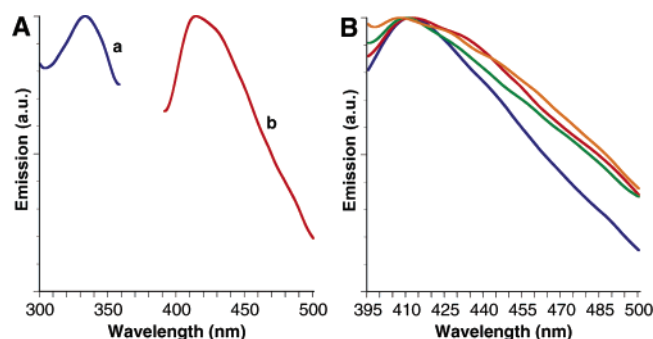


Figure 7. Spectroscopic features of samples obtained by ultracentrifugation of the pCNT sample from Carbolex, Inc. (A) Normalized excitation (trace a) and emission (trace b) spectra of the supernate obtained by ultracentrifugation of pCNT dispersed in 1% SDS. (B) Normalized emission spectra of the supernatant fractions obtained by ultrafiltration through nominal molecular weight cutoff membranes (blue, <3 kDa; red, 3–10 kDa; green, 10–30 kDa; orange, 30–100 kDa) of pCNT dispersed in 1% SDS.

TABLE 3: Emission Peak Wavelength (λ_{em}) of the Supernate and the Nominal Molecular Weight Cutoff Fractions Isolated from PCNT from Carbolex, Inc

samples ^a		λ_{em} (nm) ($\lambda_{ex} = 335$ nm)
supernate		414
fractionated supernate	30–100 kDa	407
	10–30 kDa	410
	3–10 kDa	412
	<3 kDa	413

^a Supernate obtained by ultracentrifugation at 120 000g and then fractionated by ultrafiltration.

Excitation of the clear grayish pCNT-in-SDS-derived supernate at 335 nm (Figure 7A, trace a) produced a 414-nm emission peak characterized by a shoulder at approximately 433 nm (Figure 7A, trace b).

CNT were absent from all fractions on the basis of their lack of CNT visible absorptions. Upon excitation at 335 nm, the photoemission spectra produced by pCNT-in-SDS-derived supernatant fractions exhibited maxima within a 6-nm range (407–413 nm) and were progressively weaker and blue-shifted with increasing molecular weight (Figure 7B and Table 3). Only the 3–10 and 30–100 kDa fractions showed a clear shoulder at approximately 435 nm. Emission spectra were recorded after having matched the absorptions at the 335-nm excitation wavelength for all the fractions.

3.4. Analysis of the Fluorescent Particles Isolated from the Carbon Solutions Samples. To better understand the nature of the FP we recorded HRTEM pictures and ran EDX analysis of the FP isolated from the carbon nanotubes purchased from Carbon Solutions, Inc. HRTEM imaging showed that the fractions from the pCNT-in-SDS supernate contained FP with a maximal lateral dimension that was less than 10 nm and slightly molecular-weight-dependent (Figure 8A). EDX analysis of the fractions revealed that the FP were composed mainly of calcium and zinc.

The FP in the oxCNT-in-SDS supernatant fractions ranged from approximately 70 nm in the 30–100 kDa fraction (Figure 8B) to approximately 20 nm in the <3 kDa fraction (Figure 8C) and were composed mainly of calcium, zinc, chromium, and phosphorus. Most fractions also contained some 10-nm FP (Figure 8D), which were mainly composed of calcium and chromium. Some samples also contained a fibrous material (Figure 8E) as reported by Xu et al.² Comparable fractions from the oxCNT-in-water supernate contained FP that appeared more granular and larger than in the fractions from oxCNT in SDS (Figure 8F) and were mainly composed of calcium, phosphorus, and zinc. We observed both oxygen and carbon peaks in all the recorded EDX spectra.

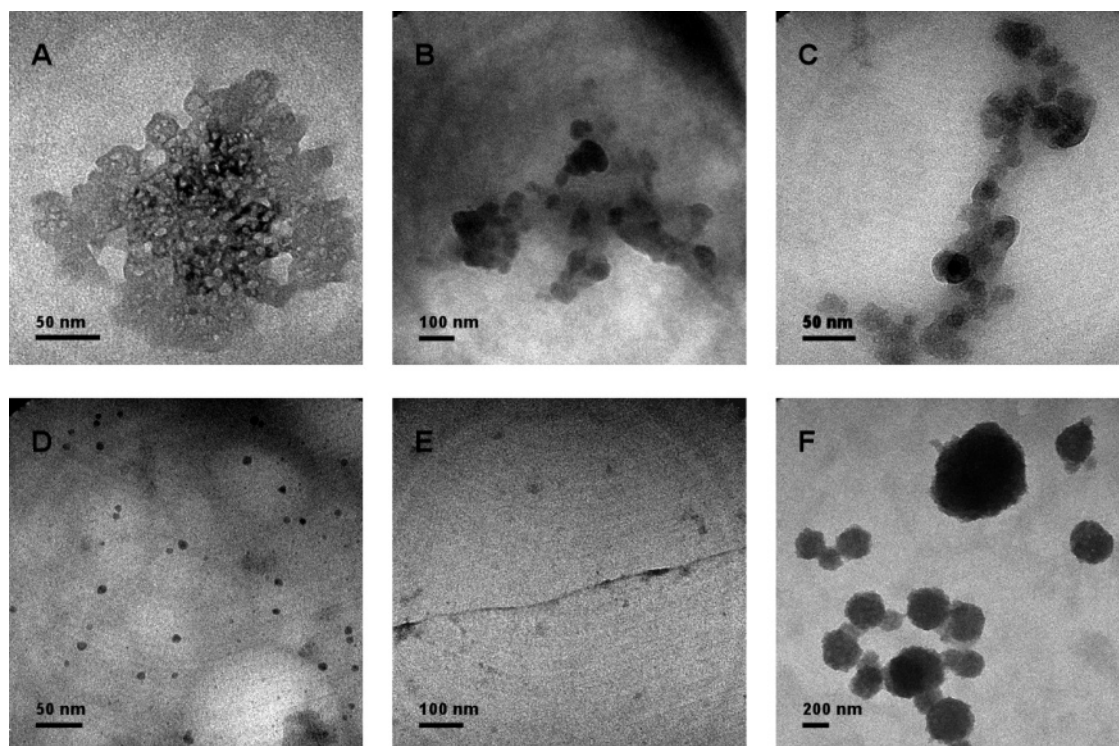


Figure 8. HRTEM images of fluorescent material from CNT (Carbon Solutions, Inc.)-derived molecular weight fractions: (A) pCNT-in-SDS <3 kDa fraction; (B) oxCNT-in-SDS 30–100 kDa fraction; (C) oxCNT-in-SDS <3 kDa fraction; (D and E) oxCNT-in-SDS 3–10 kDa fraction; (F) oxCNT-in-water <3 kDa fraction.

4. Discussion

The 420-nm photoluminescence of single-walled CNT was reported to originate from the excitation of the benzene, naphthalene, or other polyaromatic substructures in their walls.⁶ Our graphite, carbon black, and CNT samples exhibited this 420-nm peak and other emission peaks that are characteristic of graphitic material. On this basis, any other photoluminescence from the CNT samples presumably arose from extraneous fluorescent materials or nanoparticles (FP). These particles likely come from the impurities present in the graphite rods used for the production of the CNT. The photoluminescence from irradiation of the analyzed electric arc-produced CNT samples was dependent on the chemical form of the CNT (pristine or oxidized) suggesting that different forms of fluorescent contaminants were present in each sample: the pristine CNT exhibited a photoluminescence in the violet-blue range, whereas the oxidized CNT exhibited a photoluminescence ranging from blue to yellowish-green.

We conducted cup–horn sonication followed by ultracentrifugation of CNT-in-SDS dispersions in order to isolate the FP. The parameters of sonication (duration and power) and ultracentrifugation (duration and speed) were chosen in order to minimize the presence of CNT in the supernates. The collected clear supernates from the processed pCNT and oxCNT were slightly grayish and brownish, respectively, and lacking of CNT as suggested by the absence of absorption features in the visible range. More powerful and/or longer sonication and slower ultracentrifugation led to an enrichment of CNT in the supernates as revealed by their darker gray color and by the CNT-associated spectral structures in the absorbance spectra. The supernates obtained by ultracentrifugation were fractionated by ultrafiltration through nominal molecular weight cutoff membranes. The photoluminescence of the pCNT-derived fractions was less molecular-weight-dependent than that of the corresponding oxCNT-derived fractions. Moreover, the molecular weight dependency for both the pristine and oxidized CNT-derived fractions was strongly related to the specific supplier. The predominant FP in the pCNT (Carbon Solutions, Inc.)-in-SDS-derived supernate had a mean molecular weight below 30 kDa, a 315-nm excitation wavelength, and mainly violet-blue photoluminescence. In contrast, the 30–100 kDa fraction had a weaker spectrum indicating fewer FP. The photoluminescent response of the FP from the oxCNT (Carbon Solutions, Inc.)-in-SDS supernatant fractions was more size-dependent and ranged from greenish-blue to yellowish-green with increasing molecular weight. The spectrum of the <3 kDa oxCNT-in-SDS fraction showed a 425-nm emission upon excitation at 315 nm suggesting the presence of a less abundant FP fraction. The predominant FP in the pCNT (Nanocs, Inc.)-in-SDS-derived supernate had a mean molecular weight below 10 kDa, a 320-nm excitation wavelength, and mainly blue photoluminescence. In contrast, the 10–30 and 30–100 kDa fractions had weaker spectra. The predominant FP in the oxCNT (Nanocs, Inc.)-in-SDS-derived supernate had a mean molecular weight below 10 kDa, and both the excitation and emission wavelengths were size-dependent. In particular, the below 3 kDa fraction exhibited a 330-nm excitation wavelength and a 450-nm photoluminescence, whereas the 3–10 kDa fraction exhibited a 365-nm excitation and a 515-nm photoluminescence. The 10–30 and 30–100 kDa fractions had weaker spectra. The predominant FP in the pCNT (Carbolex, Inc.)-in-SDS-derived supernate had a mean molecular weight below 10 kDa, a 335-nm excitation wavelength, and a violet-blue, slightly molecular-weight-dependent photoluminescence.

Both pristine and oxidized CNT samples from one supplier (Carbon Solutions, Inc.) were treated by cup–horn sonication in both water and 1% SDS, then ultracentrifuged. The oxCNT-in-SDS-derived supernates exhibited a photoluminescence more intense with respect to the corresponding CNT-in-water-derived supernates, with matching absorption at the same excitation wavelength; moreover, the pCNT-in-water-derived supernate did not fluoresce at all. The quenching of the FP photoluminescence in the aqueous (both pristine and oxidized) CNT-derived supernates could be explained by the attachment of the FP as aggregates or occlusions onto the CNT walls. Sonication in the presence of the surfactant SDS was able to enrich the solution by solubilizing the FP into micelles. The total absence of fluorescence of the pCNT-in-water-derived supernate indicates the absence of FP in that supernate and, therefore, the higher hydrophobicity of the related FP with respect to those present in the oxCNT sample.

HRTEM images and EDX analysis on FP isolated from CNT (Carbon Solutions, Inc.) suggested that our spectral results might be due to the different dimensions and compositions of the nanoparticles. FP from pCNT had a maximal lateral dimension below 10 nm, whereas FP from oxCNT contained similarly sized FP but also much larger ones. Additionally, oxygen and carbon peaks in the EDX of the oxCNT-in-water supernatant fractions suggest that the oxCNT-derived FP were superficially oxidized and/or coated by a thin layer of carbon.⁷ These results could be explained by nitric acid treatment causing aggregation of the pCNT-derived FP, leading to larger particles in the oxCNT samples, and moreover, it could have introduced functional groups on the surface of oxCNT-derived FP, explaining their higher hydrophilicity. FP from oxCNT in water were larger and more granular with respect to those from oxCNT in SDS, probably because in the absence of surfactant, the FP hydrophobically aggregated exposing to the water only the oxidized parts of the surface.

5. Conclusions

We isolated, fractionated by molecular weight, and characterized FP from pCNT and oxCNT received from several suppliers. These FP were responsible for the photoluminescence of electric arc-produced CNT in the visible range and were likely composed of impurities that were present in the graphite rods used for the production of the CNT. Spectroscopic analysis of the samples revealed some common supplier-independent features, specifically that the FP derived from the pCNT exhibited a violet-blue photoluminescence, whereas the FP derived from the oxCNT exhibited photoluminescence ranging from blue to yellowish-green. In contrast, the molecular weight dependency for both the pristine and oxidized CNT-derived fractions was strongly related to the specific supplier. This can be explained by differing fabrication processes leading to different physical and chemical aggregation of the impurities present in the graphite rod.

We recorded HRTEM images and EDX analysis of the FP isolated from the CNT (Carbon Solutions, Inc.)-derived molecular weight fractions. The FP derived from the pCNT exhibited a narrow range in width, whereas the FP derived from the oxCNT were larger, had a broader width range, and formed hydrophilic aggregates in water. Moreover, EDX analysis of the fractions from the oxCNT-in-water supernate suggested that their FP were superficially oxidized and/or coated by a thin carbon layer.

Acknowledgment. This work was supported by Grant U54 CA119335 from the National Institutes of Health. We thank Solution Dispersions, Inc. for having generously provided the samples of carbon black and graphite. We thank Karena Kosco (Burnham Institute for Medical Research) for helpful comments.

References and Notes

- (1) (a) Baughman, R. H.; Zakhidov, A. A.; de Heer, W. A. *Science* **2002**, *297*, 787–92. (b) Lin, Y.; Lu, F.; Tu, Y.; Ren, Z. *Nano Lett.* **2004**, *4*, 191. (c) Barone, P. W.; Baik, S.; Heller, D. A.; Strano, M. S. *Nat. Mater.* **2005**, *4*, 86–92. (d) Meng, J.; Kong, H.; Xu, H. Y.; Song, L.; Wang, C. Y.; Xie, S. S. *J. Biomed. Mater. Res., Part A* **2005**, *74*, 208–14. (e) Kam, N. W.; Dai, H. *J. Am. Chem. Soc.* **2005**, *127*, 6021–6.
- (2) Xu, X.; Ray, R.; Gu, Y.; Ploehn, H. J.; Gearheart, L.; Raker, K.; Scrivens, W. A. *J. Am. Chem. Soc.* **2004**, *126*, 12736–7.
- (3) Journet, C.; Maser, W. K.; Bernier, P.; Loiseau, A.; Lamy de la Chapelle, M.; Lefrant, S.; Deniard, P.; Lee, R.; Fischer, J. E. *Nature* **1997**, *388*, 756–8.
- (4) Itkis, M. E.; Perea, D. E.; Niyogi, S.; Rickard, S. M.; Hamon, M. A.; Hu, H.; Zhao, B.; Haddon, R. C. *Nano Lett.* **2003**, *3*, 309–14.
- (5) Liu, J.; Rinzler, A. G.; Dai, H.; Hafner, J. H.; Bradley, R. K.; Boul, P. J.; Lu, A.; Iverson, T.; Shelimov, K.; Huffman, C. B.; Rodriguez-Macias, F.; Shon, Y.; Lee, T. R.; Colbert, D. T.; Smalley, R. E. *Science* **1998**, *280*, 1253.
- (6) Alvaro, M.; Atienzar, P.; Bourdelande, J. L.; Garcia, H. *Chem. Commun.* **2002**, *21*, 3004–5.
- (7) Oxygen and carbon peaks were also detected in the EDX spectra of both pCNT-in-SDS and oxCNT-in-SDS supernatant fractions; however, in these cases they could also have originated from the SDS, which exhibited similar peaks.